# PARP6, a mono(ADP-ribosyl) transferase and a negative regulator of cell proliferation, is involved in colorectal cancer development

HANDAN TUNCEL[1], SHINJI TANAKA[2], SHIRO OKA[2], SHIRO NAKAI[3], RYUICHIRO FUKUTOMI[4], MAYUMI OKAMOTO[4], TAKAHIDE OTA[5], HIROSHI KANEKO[6], MASAAKI TATSUKA[4] and FUMIO SHIMAMOTO[6]

[1]Department of Biophysics, Cerrahpasa Medical Faculty, Istanbul University, Istanbul 34303, Turkey; [2]Department of Endoscopy, Hiroshima University Hospital, Minami-ku, Hiroshima 734-8553; [3]Department of Surgery, Hiroshima Memorial Hospital, Naka-ku, Hiroshima 730-0802; [4]Department of Life Sciences, Faculty of Life and Environmental Sciences, Prefectural University of Hiroshima, Shoubara, Hiroshima 727-0023; [5]Department of Life Sciences, Medical Research Institute, Kanazawa Medical University, Uchinada, Ishikawa 920-0293; [6]Department of Health Sciences, Faculty of Human Culture and Science, Prefectural University of Hiroshima, Minami-ku, Hiroshima 734-8558, Japan

Received July 11, 2012; Accepted August 28, 2012

DOI: 10.3892/ijo.2012.1652

**Abstract.** Poly(ADP-ribose) polymerase (PARP) is an enzyme that mediates post-translational modification of proteins. Seventeen known members of the PARP superfamily can be grouped into three classes based on catalytic activity: (i) classical poly(ADP-ribose) polymerases, (ii) mono(ADP-ribosyl) transferases and (iii) catalytically inactive members. PARP6 belongs to the mono(ADP-ribosyl) transferase class, and here we have found that PARP6 is a negative regulator of cell proliferation. Forced expression of PARP6 in HeLa cells induced growth suppression, but a PARP6 mutant with a C-terminal deletion lacking the catalytic domain had no effect. The PARP6-expressing cells accumulated in the S-phase, and the magnitude of S-phase accumulation was observed to be greater in cells expressing a PARP6 mutant with an N-terminal deletion, lacking a putative regulatory domain. Immunohistochemical analysis revealed that PARP6 positivity was found at higher frequencies in colorectal cancer tissues with well-differentiated histology compared to those with poorly differentiated histology. Furthermore, PARP6 positivity negatively correlated with the Ki-67 proliferation index. Kaplan-Meier analysis showed that PARP6-positive colorectal cancer had a good prognosis. Based on these results, we propose that PARP6 acts as a tumor suppressor through its role in cell cycle control.

*Correspondence to:* Professor Fumio Shimamoto, Department of Health Sciences, Faculty of Human Culture and Science, Prefectural University of Hiroshima, 1-1-71 Ujina-Higashi, Minami-ku, Hiroshima 734-8558, Japan
E-mail: simamoto@pu-hiroshima.ac.jp

Professor Masaaki Tatsuka, Laboratory of Radiation Genome Systems Biology, Department of Life Sciences, Faculty of Life and Environmental Sciences, Prefectural University of Hiroshima, 562 Nanatsuka, Shoubara, Hiroshima 727-0023, Japan
E-mail: tatsuka@pu-hiroshima.ac.jp

*Key words:* poly(ADP-ribose) polymerase 6, colorectal cancer, cell proliferation and prognosis

## Introduction

Post-translational protein modification by poly(ADP-ribosyl)ation is involved in a variety of biological processes including chromatin structural regulation, transcription, DNA repair, DNA replication, telomere homeostasis, cell division, cell proliferation, cell death and other physiological and pathological functions (1-5). The reactions are catalytically mediated by poly(ADP-ribose) polymerases(PARPs). Recent studies indicated that there are 17 members of the PARP superfamily (6).

By comparing the catalytic domain structures of these 17 members, three different classes of PARP proteins have been defined (7). The first subfamily consists of enzymes that have been demonstrated or structurally predicted to catalyze poly(ADP-ribosyl)ation. PARP1, PARP2, PARP3, PARP4, PARP5a and PARP5b belong to this subfamily. The second subfamily members (PARP6, PARP7, PARP8, PARP10, PARP11, PARP12, PARP14, PARP15 and PARP16) have a considerably shorter nicotinamide-ribose-binding site than PARP1, thus these enzymes have been structurally predicted to catalyze mono(ADP-ribosyl)ation. Indeed, the first analyzed enzyme belonging to this subfamily, PARP10, has been demonstrated to be a mono(ADP-ribosyl) transferase with auto-mono(ADP-ribosyl)ation activity (7). The third subfamily members (PARP9 and PARP13) lack the $\beta$-NAD$^+$ cofactor-binding domain.

Among PARPs, the members capable of mediating poly(ADP-ribosyl)ation have been extensively examined physiologically, but the biological functions of the mono(ADP-ribosyl) transferase subfamily members are largely unexplored.

Several limited studies suggested the involvement of mono(ADP-ribosyl) transferases in growth control (7-13), opening new areas for investigation. PARP10 was identified as a novel protein that interacts with Myc oncoproteins (13). When expressed in rat embryo fibroblasts, oncogenic transformation induced by c-Myc plus Ha-Ras expression was inhibited (13). Also, the growth rate was reduced by PARP10 expression in HeLa cells (7). PARP10 phosphorylation by cyclin-dependent kinases was suggested to be its cell cycle regulation mechanism (10). PARP14 was identified as a novel modification protein that stabilizes autocrine motility factor (AMF)/phosphoglucose isomerase (12). PARP14 is also known as a regulator of Stat6 transcription activity, which leads to the transduction of cell survival signals (8,9,11).

We analyzed PARP6 and found that it is involved in negative regulation of cell cycle progression. When expressed in HeLa cells, cell proliferation was inhibited depending on the PARP6 catalytic domain, which is highly conserved among vertebrates. Immunohistochemical analysis of human colorectal cancer specimens demonstrated that PARP6 protein expression was inversely correlated with Ki-67 positivity and was linked to a good prognosis. To our knowledge, this is the first demonstration that PARP6 controls cancer cell growth.

## Materials and methods

*Cell lines and cell culture*. The human cervical cancer cell line, HeLa, was provided by the late Professor Masakatsu Horikawa, Faculty of Pharmaceutical Sciences, Kanazawa University (Kanazawa, Japan) (14). HEK293FT cells were purchased from Life Technologies, Japan. Cells were cultured in Dulbecco's modified Eagle's medium containing 10% fetal bovine serum, penicillin (50 U/ml) and streptomycin (50 $\mu$g/ml), at 37˚C in a humidified atmosphere of 5% $CO_2$ and 95% air.

*Patients and tissue samples*. A total of 126 advanced colorectal carcinomas (72 men and 54 women), including 62 cases with lymph node metastasis and 24 cases with distant metastasis, were obtained from the archive of Hiroshima University Hospital during 1984-2001 after surgical resection. The age range was 37-84 years (mean, 64.3 years). Tissues were fixed in 10% buffered formalin and embedded in paraffin. The study protocol followed the ethical guidelines of Hiroshima University and Prefectural University of Hiroshima. Informed consent was obtained from all subjects.

*Plasmids and transfection*. A full-length cDNA clone encoding PARP6 (BC110902) was subcloned into a pEGFP vector (pEGFP-PARP6) to produce an enhanced green fluorescent protein (EGFP)-tagged protein. cDNA clones encoding two alternative splicing forms (AB499727 and AB499728) were also subcloned into a pEGFP vector (pEGFP-PARP6-SP1 and pEGFP-PARP6-SP2). An N-terminal deletion mutant (deletion of 410 amino acid residues) was also constructed [pEGFP-ΔN(1-410)PARP6]. Transfection was performed using Lipofectamine 2000 (Life Technologies) according to the manufacturer's guidelines.

*Cell growth assay*. Proliferation activity was measured by the water-soluble tetrazolium-1 reagent assay (WST-1, Roche Applied Science) in transiently transfected cells, according to the manufacturer's protocol. HeLa cells were transfected with pEGFP-empty, pEGFP-PARP6, pEGFP-PARP6-SP1 or pEGFP-PARP6-SP2. Transfection efficiencies were >80% as confirmed by EGFP expression under a fluorescence microscope. After 24 h, transfected cells were replated in 96-well plates. WST-1 assay was performed at each time point (1, 2 and 3 days) and the values were expressed as a percentage change.

*DNA histograms*. Cells were transfected with pEGFP-empty, pEGFP-PARP6 or pEGFP-ΔN(1-410)PARP6. After 24 h, the transfected cells were fixed with 20% ethanol and incubated with 0.1% RNase (Type II-A, Sigma-Aldrich, Japan) for 30 min at 37˚C. The cells were stained with propidium iodide (50 $\mu$g/ml), and green (for EGFP) and red (for propidium iodide) fluorescence from individual cells were measured using a FACSort flow cytometer (BD Biosciences).

*Immunoblot analysis*. Transfected cells were lysed with ice-cold Laemmli sodium dodecyl sulfate (SDS)-sample buffer (pH 6.8), consisting of 25 mM Tris-HCl, 5% glycerol, 2.5% 2-mercaptoethanol and 1% SDS, containing protease inhibitor cocktail (Sigma-Aldrich). The lysates were sonicated three times for 10 sec on ice and centrifuged at 15,000 rpm for 1 min at 4˚C. The supernatant was collected and the protein concentration was determined using the Bio-Rad protein assay kit (Bio-Rad Laboratories). Equal amounts of protein (20 $\mu$g per lane) were loaded on a 10% SDS-polyacrylamide gel. The cell lysates were resolved by electrophoresis and transferred to Immobilon-P membranes (Merck Millipore). Membranes were blocked with skim milk, probed with primary antibodies, washed and then incubated with secondary antibody. Anti-GFP antibody (JL-8, Clontech Laboratories), anti-α-tubulin (CLT9002, Cedarlane Laboratories) and anti-β-actin (A1978, Sigma-Aldrich) were used as primary antibodies. Horseradish peroxidase-conjugated anti-mouse antibody (GE Healthcare, Japan) was used as secondary antibody. Proteins were visualized on X-ray film using ECL Western Blotting Detection Reagent (GE Healthcare).

*Immunohistochemical analysis*. For immunohistochemical examination, serial 4-$\mu$m sections were stained with hematoxylin and eosin and used for immunohistochemical analysis. Immunohistochemical staining was carried out with anti-PARP6 antibody (HPA026991, Sigma-Aldrich), raised against the PARP6 catalytic domain (497-589), after antigen retrieval by microwave treatment in citrate buffer (pH 6.0) and detection was performed by the streptavidin-biotin peroxidase system (Universal LSAB™2 kit, Dako, Japan). This PARP6 antibody is specific to PARP6, but does not recognize PARP6-SP1 and PARP6-SP2. In addition, to determine the proliferative cell activity and correlate it with PARP6 expression, we examined Ki-67 expression using anti-Ki-67 monoclonal antibody (MIB-1, Dako). The sections were incubated with primary antibodies at 4˚C overnight. The immunostaining was defined as positive when >20% of the tumor cells were stained for PARP6 in the cytoplasm. The immunohistochemistry grade was defined as - to +++ according to the number of cells stained and to the intensity of the reaction in individual cells. Grades were defined as follows: -, mostly no positive cells; +, 5-20% of tumor cells

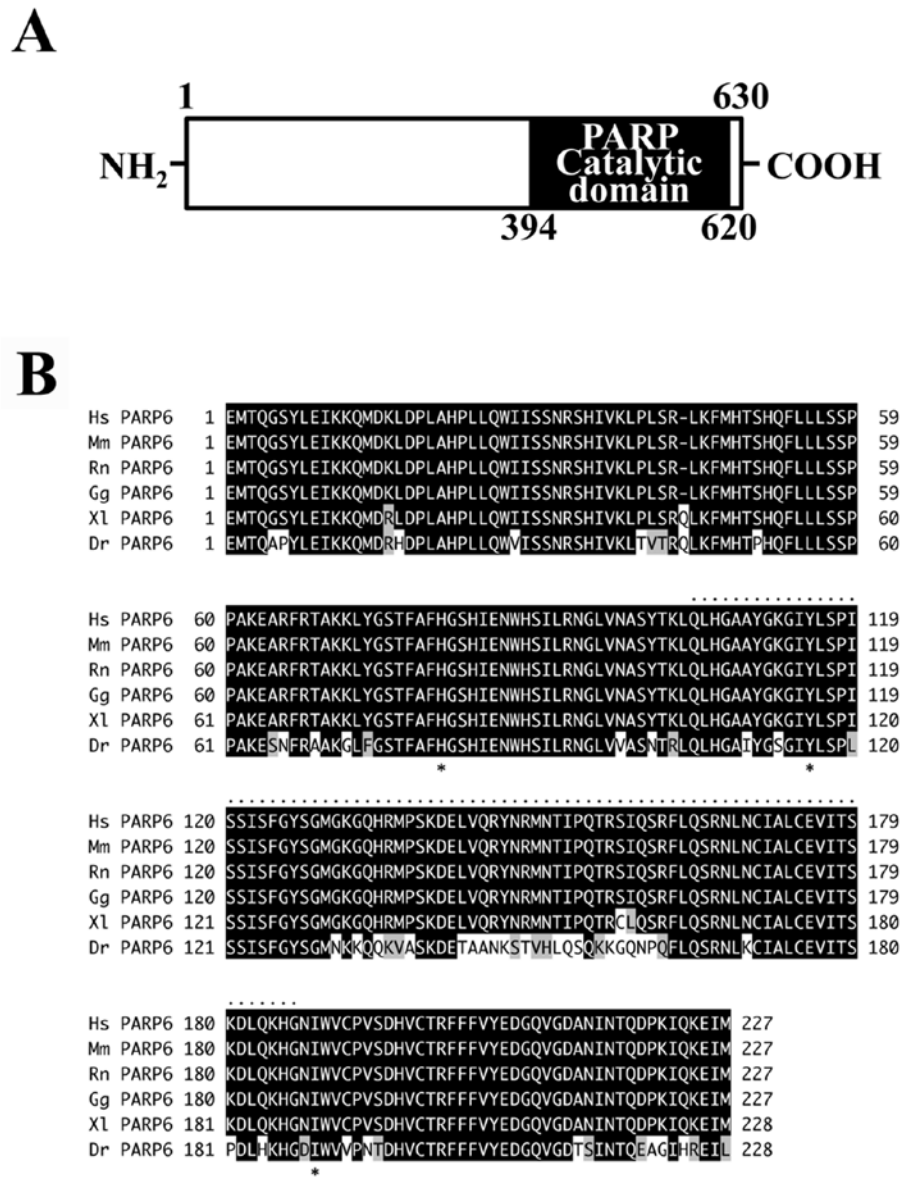


Figure 1. Amino acid sequences of PARP6 proteins, belonging to the mono(ADP-ribosyl) transferase subfamily. (A) A schematic illustration of the human PARP6 protein. PARP6 consists of 630 amino acid residues and has a PARP catalytic domain, which is composed of 227 amino acids in the C-terminal region. (B) Multiple sequence alignment of the vertebrate PARP6 catalytic domain, which is highly conserved among vertebrates. Black shading indicates identical amino acid residues, and halftone shading indicates related amino acid residues. Asterisks indicate the residues of the conserved 'HYI' triad within the mono(ADP-ribosyl) transferase catalytic domain. Dots indicate the immunogen sequence for the polyclonal antibody against PARP6. Genes consisting of a PARP6 domain cannot be found in invertebrates.

showed weak to moderate immunoreactivity; ++, 20-50% of tumor cells showed moderate immunoreactivity; +++, over 50% of tumor cells showed intense immunoreactivity. Cases with grade ++ and +++ were regarded as positive cases. A labeling index percentage of Ki-67-positive cells was determined by examining at least 1,000 tumor cells at x200 magnification in five representative areas.

*Statistical analysis*. The Statcel software package (KaleidaGraph Version 4.1) was used for analysis. The $\alpha^2$ test and Fisher's and t-test (Statcel - The useful Addin Forms on Excel - 2nd edition) were used for comparison of data between two groups. Survival analysis was conducted according to the Kaplan-Meier method and survival characteristics and were compared using log-rank tests. A $P<0.05$ was considered to indicate statistical significance.

## Results

*PARP6 expression inhibits cell growth*. Full-length PARP6 consists of 630 amino acids with a molecular mass of approximately 71 kDa. The C-terminal region (residues 394-620) contains the PARP catalytic domain (Fig. 1A). Database analysis revealed the presence of a putative PARP6 in vertebrates but not in invertebrates. Within vertebrates, the catalytic domain of PARP6 is highly conserved; in human, mouse, rat and chicken it is completely identical, and in frog and fish it is 98 and 78% identical, respectively (Fig. 1B). The

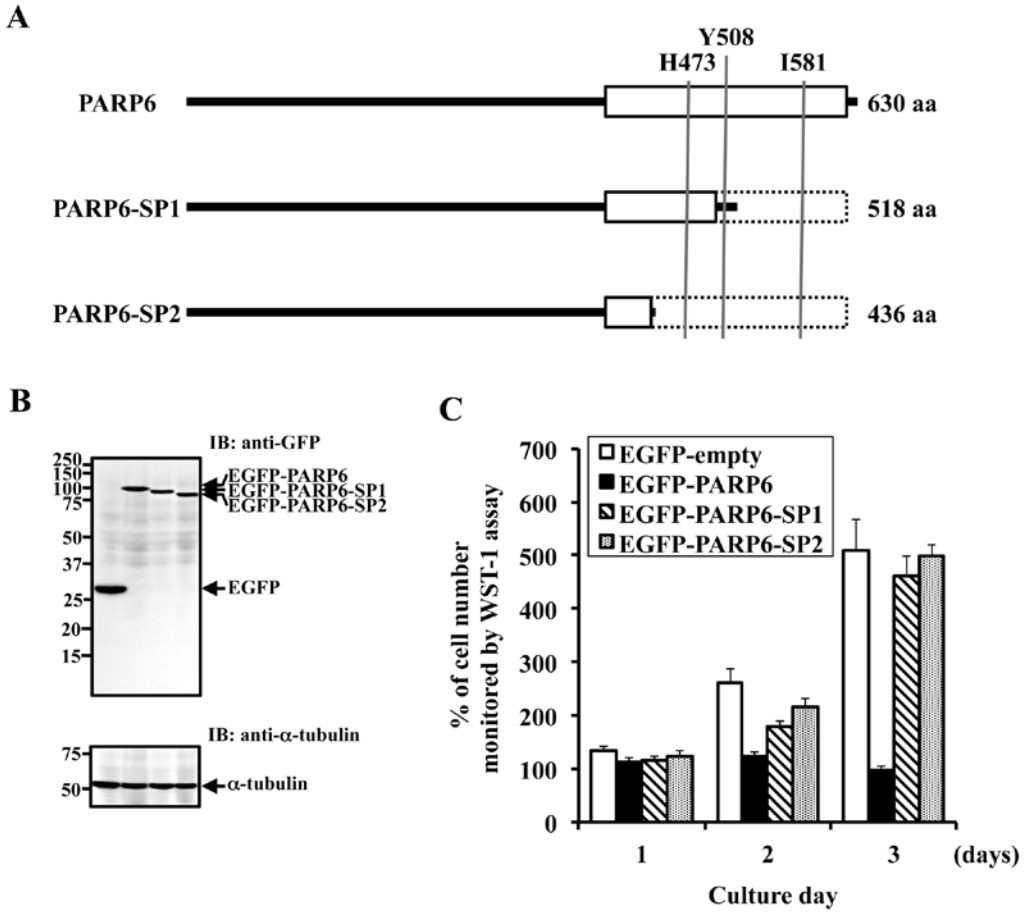


Figure 2. Cell growth inhibition by PARP6. (A) Schematic illustration of the catalytic domain structures of PARP6 and its alternatively spliced forms (PARP6-SP1 and PARP6-SP2). PARP6-SP1 lacks the Y and I residues within the conserved 'HYI' triad, and PARP6-SP2 lacks all three residues. (B) Expression of PARP6 and its splicing variants in HeLa cells was examined by immunoblot analysis. Expression vectors (pEGFP-empty, pEGFP-PARP6, pEGFP-PARP6-SP1 and pEGFP-PARP6-SP2) were transfected into HeLa cells. After 24 h, cells were lysed and immunoblotting was performed. (C) Cell growth was measured by the WST-1 reagent. Cells were replated 24 h after transfection and were cultured for one, two and three days. WST-1 assay was performed, and the values are expressed as a percentage change. Transfection efficiencies were >80% as confirmed by EGFP expression under a fluorescence microscope. Values indicate mean ± SD (n=3).

residues of the conserved 'HYI' triad, which is critical for the mono(ADP-ribosyl)ation catalytic activity, are widely present in vertebrates (Fig. 1B).

During the PARP6 cDNA screening in cDNA libraries from HeLa cells and SW480 cells, we noticed that the full-length PARP6 expression was extremely low, and there were two alternatively spliced forms in these libraries. Both these forms, PARP6-SP1 (accession number AB499727) and PARP6-SP2 (accession number AB499728), lack the critical structure of the PARP catalytic domain (Fig. 2A). To clarify the effects of PARP6 expression on cell growth, HeLa cells were transfected with plasmids (pEGFP-PARP6, pEGFP-PARP6-SP1 or pEGFP-PARP6-SP2) to express EGFP-tagged PARP6 proteins (Fig. 2B). The data clearly revealed that cell growth was inhibited by full-length PARP6 expression (Fig. 2C). On the other hand, EGFP-PARP6-SP1 and EGFP-PARP6-SP2, which are catalytically inactive, had no effect on cell growth (Fig. 2C). These results clearly indicate that the PARP6 catalytic domain is essential for PARP6-mediated cell growth inhibition.

*PARP6 expression inhibits S-phase progression*. Next, we examined whether PARP6 blocks cell cycle progression at a specific cell cycle phase. In PARP proteins, the N-terminal region plays a role in the regulation of the catalytic activity. Therefore, we constructed an expression vector encoding an N-terminal deletion form of PARP6 (Fig. 3A). HEK293FT cells, which like HeLa cells express extremely low levels of PARP6, were transfected with plasmids [pEGFP-PARP6 or pEGFP-ΔN(1-410)PARP6] to express EGFP-tagged full-length and N-terminal-deleted PARP6 proteins. Cells were harvested 24 h after transfection, and cell cycle distribution and expression level of the transfected plasmid were analyzed by flow cytometry (Fig. 3B). In low-level-expressing cells (Gate A in Fig. 3C), the S-phase cell populations were 29.79, 34.40 and 44.76% for EGFP-empty-expressing cells, EGFP-PARP6-expressing cells and EGFP-ΔN (1-410)PARP6-expressing cells, respectively. In moderate-level-expressing cells (Gate B in Fig. 3C), over 90% of EGFP-ΔN (1-410) PARP6-expressing cells were accumulated in the S-phase. In high-level-expressing cells (Gate C in Fig. 3C), over 60% of EGFP-PARP6-expressing cells were accumulated in the S-phase. Thus, the expression of PARP6 induced S-phase arrest. The magnitude of S-phase accumulation was greater in EGFP-ΔN (1-410) PARP6-expressing cells than in EGFP-PARP6-expressing cells. Thus, the PARP6

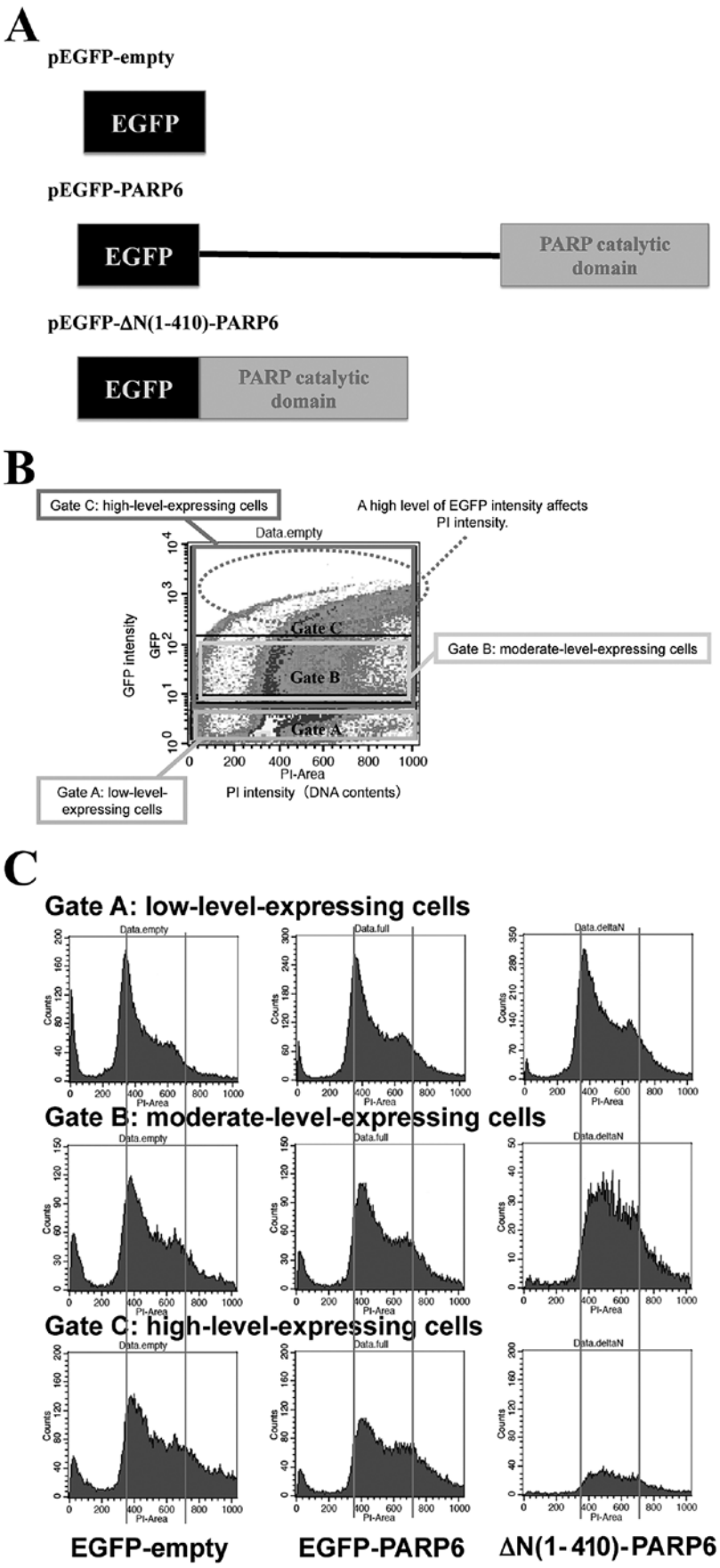


Figure 3. Inhibition of cell cycle progression by PARP6. (A) A schematic illustration of the recombinant proteins produced from expression vectors used for cell cycle analysis [pEGFP-empty, pEGFP-PARP6 and pEGFP-ΔN(1-410)PARP6]. (B) A typical example of a two-parameter histogram is shown as a dot plot displaying PI intensity (DNA contents; x-axis) and GFP intensity (y-axis). Based on the GFP intensity, the cell population was divided into three groups for gating. (C) DNA histograms were measured 24 h after transfection of HEK293FT cells with the plasmids shown in (A). The data are displayed as histograms of each gating group as shown in (B). Transfection efficiencies were >80% as confirmed by EGFP expression under a fluorescence microscope.

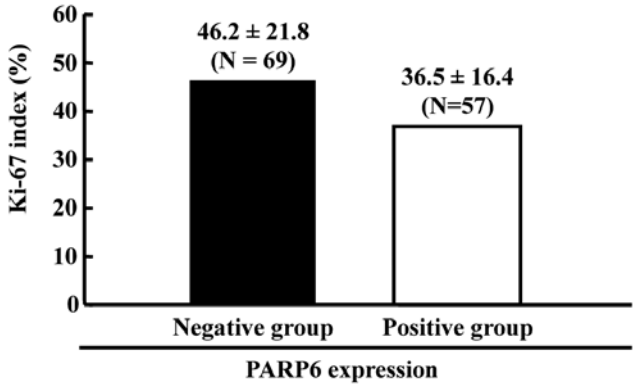


Figure 4. Negative relationship between PARP6 expression and proliferation marker Ki-67 expression in colorectal cancers. PARP6 positivity was examined by immunohistochemical analysis. We found that colorectal cancerous tissues divided into two groups, the PARP6-positive group and the PARP6-negative group. The frequencies of Ki-67-positive cells were compared between the groups. The Ki-67 index was significantly higher in the PARP6-negative group (46.2±21.8%) than in the PARP6-positive group (36.5±16.4%; P<0.01).

catalytic domain is likely to have an important role in inhibition of S-phase progression.

*PARP6 expression correlates with a good prognosis in colorectal cancer.* Because PARP6 functioned as a cell growth inhibitor, we decided to explore the possibility that PARP6 may act as a tumor suppressor in human cancer. The expression level of PARP6 was examined in 126 colorectal cancer cases by immunohistochemistry, using PARP6 antibody against the catalytic domain. We observed that 57 (45.6%) cases were positive. Among these 126 cases, the frequency of proliferation marker Ki-67-positive cells was higher in PARP6-negative cases than in PARP6-positive cases (Fig. 4). Thus, we confirmed that PARP6 negatively regulates cell growth in colorectal cancerous tissues.

We also observed PARP6 positivity especially in the cytoplasm of well-differentiated and moderately differentiated adenocarcinoma, but hardly any in poorly differentiated adenocarcinoma and mucinous carcinoma (Fig. 5). PARP6 positivity was inversely correlated with loss of histological differentiation (P<0.01; Table I). The correlation between PARP6 positivity and other clinicopathological factors was also examined, and we found that in primary colorectal cancer with distant metastasis (P<0.01) and with stage D (P<0.01) the PARP6-negative cases were significantly higher than the PARP6-positive cases (Table I).

To determine whether PARP6 expression is emerging as a prognostic biomarker for survival in colorectal cancer patients, we examined the survival rate of those 126 cases by the Kaplan-Meier method. The patient survival curves indicated that the survival rate of PARP6-positive cases was higher than that of the negative cases (P<0.001; Fig. 6A). When the survival rate within patients with B, C or D stage was examined, we found that the 5-year-survival rate of PARP6-positive cases was higher than that of negative cases within stage C patients, and that it was not significantly different within stage B or D patients (Fig. 6B, C and D). When the survival rate within patients with differentiated or undifferentiated type cancers was examined, we found that the 5-year-survival rate of PARP6-positive cases was higher than that of negative cases within the differentiated type cases (Fig. 6E). A similar pattern was observed within the undifferentiated type cases (Fig. 6F). In conclusion, PARP6 expression may become a prognostic biomarker for colorectal cancer patient survival.

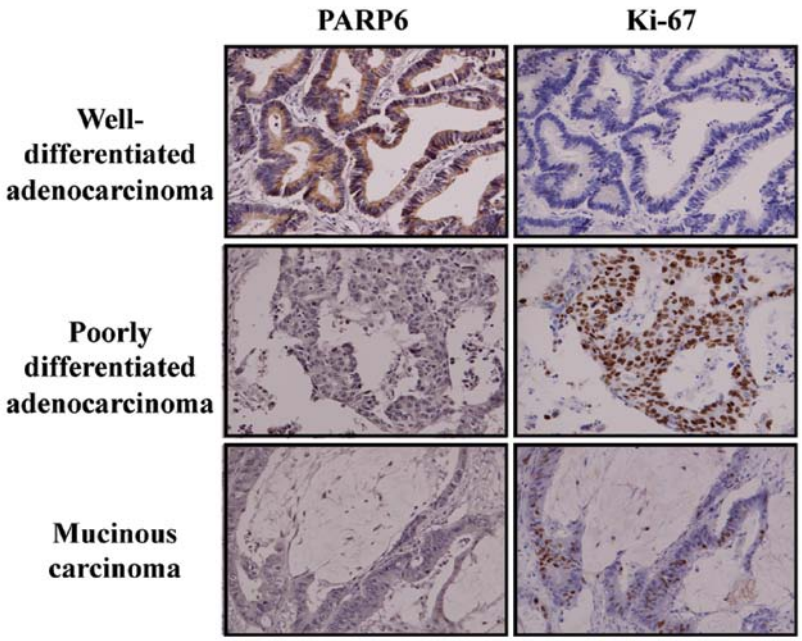


Figure 5. Immunohistochemistry of PAPR6 in well-differentiated adenocarcinoma, poorly differentiated adenocarcinoma and mucinous carcinoma. PARP6 positivity was predominantly observed in well-differentiated adenocarcinoma, but rarely observed in poorly differentiated adenocarcinoma and mucinous carcinoma (also known as a poorly differentiated cancerous tissue). Details are shown in Table I.

Table I. Correlation between PARP6 expression and clinicopathological factors in colorectal cancer.

| Clinicopathological factor | PARP6 expression | | P-value |
|---|---|---|---|
| | Negative 69 | Positive 57 | |
| Tumor size (mm) | | | |
| >50 | 32 | 24 | |
| ≤50 | 37 | 33 | |
| Histological differentiation | | | |
| Por/Muc[a] | 15 | 1 | <0.01 |
| W/M[b] | 54 | 56 | |
| Lymph node metastasis | | | |
| Negative | 30 | 34 | 0.071 |
| Positive | 39 | 23 | |
| Lymphatic invasion | | | |
| Negative | 10 | 12 | |
| Positive | 59 | 45 | |
| Venous invasion | | | |
| Negative | 25 | 23 | |
| Positive | 44 | 34 | |
| Metastasis | | | |
| Negative | 49 | 53 | <0.01 |
| Positive | 20 | 4 | |
| Tumor stage | | | |
| B, C | 46 | 51 | <0.01 |
| D | 23 | 6 | |

[a]Poorly differentiated adenocarcinoma/mucinous carcinoma; [b]well-differentiated tubular adenocarcinoma/moderately differentiated tubular adenocarcinoma.

## Discussion

To date, the 17 identified PARPs share a PARP domain and thus may contain polymerase activity (3,6,15,16). The structure- and sequence-based analyses of the PARP catalytic core motifs and the loop length (between $\beta$-sheets 4 and 5) have indicated that these PARPs can be divide into three functionally distinct subgroups according to their catalytic activity: (i) poly(ADP-ribosyl) polymerase activity, (ii) mono(ADP-ribosyl) transferase activity and (iii) catalytically inactive (7). PARP6 has a histidine (H473) and tyrosine (Y508) that are involved in $NAD^+$ binding, and an isoleucine (I581) that replaces the catalytic glutamate found in PARP1 (E988). Moreover, the loop between $\beta$-4 and $\beta$-5 is only two residues long in PARP6. These features are characteristic of mono (ADP-ribosyl) transferases. This is the first report demonstrating that PARP6 has a physiological function.

An extremely low level of PARP6 expression was found in cultured cancer cells such as HeLa cells and HEK293FT cells. We were also unable to detect PARP6 expression in cultured colorectal cancer cell lines, including SW480 cells and HCT116 cells (data not shown). On the other hand, alternatively spliced forms of PARP6 lacking parts of the catalytic domain

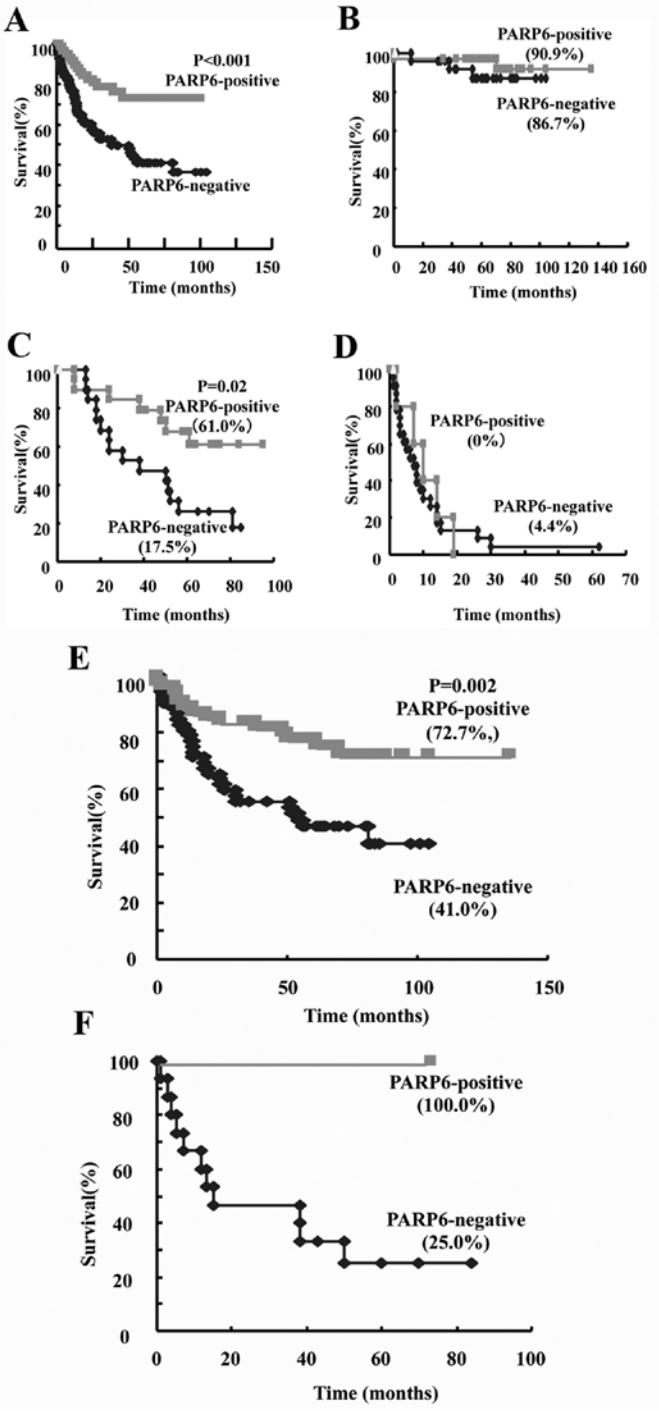


Figure 6. Kaplan-Meier survival curves of patients with colorectal cancer according to PARP6 expression. (A) All examined patients who had PARP6-positive cancer had a 5-year survival rate of 73.2%, which was significantly higher than the survival rate of patients who had PARP6-negative cancer (36.6%; P<0.001). (B) Dukes' stage B patients who had PARP6-positive cancer had a 5-year survival rate of 90.9%, which was not significantly different from the 86.7% rate of Dukes' stage B patients who had PARP6-negative cancer. (C) Dukes' stage C patients who had PARP6-positive cancer had a 5-year survival rate of 61.0%, which was significantly higher than the 17.5% rate in Dukes' stage C patients who had PARP6-negative cancer (P=0.02). (D) Dukes' stage D patients who had PARP6-positive cancer had a 5-year survival rate of 0%, which was not significantly different from the 4.4% rate of Dukes' stage D patients who had PARP6-negative cancer. (E) All examined patients who had PARP6-positive differentiated type cancer had a 5-year survival rate of 72.7%, which was significantly higher than the 41.0% rate of all examined patients who had PARP6-negative differentiated type cancer (P=0.002). (F) All examined patients who had PARP6-positive undifferentiated type cancer had a 5-year survival rate of 100%, which was higher, but not statistically significant, than the 25.0% rate of all examined patients who had PARP6-negative undifferentiated type cancer.

(PARP6-SP1 and PARP6-SP2) were found in HeLa cells as well as in other cell lines including colorectal cancer cells. It is not clear whether these alternatively spliced species are actually translated in the cells. However, forced expression of these forms had no effect on cell growth. In contrast, full-length PARP6 and an N-terminal-deleted catalytic domain inhibited cell growth, leading to S-phase accumulation. In previous studies, PARP10, a mono(ADP-ribosyl) transferase, has been demonstrated to have a growth inhibitory effect (7,10,13). It has been suggested that the direct interaction between PARP10 and Myc oncoprotein is the mechanism by which PARP10 functionally inhibits c-Myc- and Ha-Ras-induced transformation of rat embryo fibroblasts (8). Although the anti-oncogenic effect of PARP10 has been considered to be independent of PARP activity (13), mutational analysis of the PARP10 catalytic domain has implicated the catalytic activity of PARP10 in growth inhibition (13). In analogy to PARP10, the data presented in this study suggest that the catalytic activity of PARP6 is required for negative regulation of S-phase progression. Furthermore, the expression of alternatively spliced forms lacking the catalytic domain in cancer cells suggests dominant-negative effects on growth inhibition if these forms are translated.

The mechanism by which PARP6 functionally inhibits cell growth due to S-phase accumulation remains unclear. In the case of PARP10, protein expression has been detected in both the cytoplasm and nucleus, and the nuclear PARP10 is likely to be critical for its function (10). PARP14, another mono (ADP-ribosyl) transferase, has been reported as both a cytoplasmic negative regulator of the cancer metastasis-related protein, AMF (12), and as a nuclear transcription switch of Stat6-dependent gene activation (8,9,11). PARP6 was predominantly distributed in the cytoplasm of well-differentiated adenocarcinoma (Fig. 5), suggesting it has cytoplasmic target(s). Although elucidation of these molecular target(s) remains challenging, PARP6 may function in a distinct subcellular localization from PARP10 and PARP14.

In colorectal cancer, PARP6 expression was detected in 57 (45.6%) of the 126 cases. Compared to Ki-67 expression, we confirmed that PARP6 is a possible negative regulator of cell growth *in vivo* as well as *in vitro*. The absence of PARP6 would be expected to contribute to cancer progression, and indeed, our analyses indicated that its reduced expression was associated with a poor prognosis. The different incidence of PARP6 positivity between well-differentiated adenocarcinoma and poorly differentiated adenocarcinoma suggests that PARP6 functions in differentiated cells. PARP6 may serve as a novel biomarker for colorectal cancer, and our present results may provide crucial information for the creation of a novel therapeutic strategy using selective PARP inhibitors, which is now becoming a promising approach in cancer therapy.

**Acknowledgements**

This study was supported in part by the Important Research Grant from the Prefectural University of Hiroshima, Japan. We thank Saki Tomita, Hidehiko Kawai, Kenta Watanabe, Shou Miyawaki, Takahiko Tsuno, Masato Hori, Mikiko Fujii, Sanae Koya, Shou Kato, Tomohiro Doi, Satomi Koga, Tomoharu Miki and Yuki Takeshita for their technical assistance.

**References**

1. D'Amours D, Desnoyers S, D'Silva I and Poirier GG: Poly(ADP-ribosyl)ation reactions in the regulation of nuclear functions. Biochem J 342: 249-268, 1999.
2. Kim MY, Zhang T and Kraus WL: Poly (ADP-ribosyl)ation by PARP-1: 'PAR-laying' $NAD^+$ into a nuclear signal. Genes Dev 19: 1951-1967, 2005.
3. Schreiber V, Dantzer F, Ame JC and de Murcia G: Poly(ADP-ribose): novel functions for an old molecule. Nat Rev Mol Cell Biol 7: 517-528, 2006.
4. Hsiao SJ and Smith S: Tankyrase function at telomeres, spindle poles, and beyond. Biochimie 90: 83-92, 2008.
5. Kraus WL: Transcriptional control by PARP-1: chromatin modulation, enhancer-binding, coregulation, and insulation. Curr Opin Cell Biol 20: 294-302, 2008.
6. Hakme A, Wong HK, Dantzer F, *et al*: The expanding field of poly(ADP-ribosyl)ation reactions. 'Protein Modifications: Beyond the Usual Suspects' Review Series. EMBO Rep 9: 1094-1100, 2008.
7. Kleine H, Poreba E, Lesniewicz K, *et al*: Substrate-assisted catalysis by PARP10 limits its activity to mono-ADP-ribosylation. Mol Cell 32: 57-69, 2008.
8. Cho SH, Ahn AK, Bhargava P, *et al*: Glycolytic rate and lymphomagenesis depend on PARP14, an ADP ribosyltransferase of the B aggressive lymphoma (BAL) family. Proc Natl Acad Sci USA 108: 15972-15977, 2011.
9. Cho SH, Goenka S, Henttinen T, *et al*: PARP-14, a member of the B aggressive lymphoma family, transduces survival signals in primary B cells. Blood 113: 2416-2425, 2009.
10. Chou HY, Chou HT and Lee SC: CDK-dependent activation of poly (ADP-ribose) polymerase member 10 (PARP10). J Biol Chem 281: 15201-15207, 2006.
11. Mehrotra P, Riley JP, Patel R, *et al*: PARP14 functions as a transcriptional switch for Stat6-dependent gene activation. J Biol Chem 286: 1767-76, 2011.
12. Yanagawa T, Funasaka T, Tsutsumi S, *et al*: Regulation of phosphoglucose isomerase/autocrine motility factor activities by the poly(ADP-ribose) polymerase family-14. Cancer Res 67: 8682-8689, 2007.
13. Yu M, Schreek S, Cerni C, *et al*: PARP-10, a novel Myc-interacting protein with poly(ADP-ribose) polymerase activity, inhibits transformation. Oncogene 24: 1982-1993, 2005.
14. Scherer WF, Syverton JT and Gey GO: Studies on the propagation in vitro of poliomyelitis viruses. IV. Viral multiplication in a stable strain of human malignant epithelial cells (strain HeLa) derived from an epidermoid carcinoma of the cervix. J Exp Med 97: 695-710, 1953.
15. Ame JC, Spenlehauer C and de Murcia G: The PARP superfamily. Bioessays 26: 882-893, 2004.
16. Otto H, Reche PA, Bazan F, *et al*: In silico characterization of the family of PARP-like poly (ADP-ribosyl) transferases (pARTs). BMC Genomics 6: 139, 2005.